Chemical Physics Letters 683 (2017) 352–356

Contents lists available at ScienceDirect

Chemical Physics Letters

journal homepage: www.elsevier.com/locate/cplett

Research paper

A full-dimensional time-dependent wave packet study of the $H + CO_2 \rightarrow OH + CO$ reaction

Peng Sun [a,b], Jun Chen [c], Shu Liu [a,*], Dong H. Zhang [a,*]

[a] State Key Laboratory of Molecular Reaction Dynamics and Center for Theoretical Computational Chemistry, Dalian Institute of Chemical Physics, Chinese Academy of Sciences, Dalian 116023, PR China
[b] University of Chinese Academy of Sciences, Beijing 100049, PR China
[c] Xiamen University, Xiamen 361005, PR China

ARTICLE INFO

Article history:
Received 1 January 2017
In final form 27 February 2017
Available online 28 February 2017

ABSTRACT

A full dimensional quantum dynamics calculation has been carried out to study the prototypical complex forming $H + CO_2 \rightarrow OH + CO$ reaction. The total reaction probability is converged with a propagation time much shorter than the reverse reaction, and only exhibits very small oscillatory structures, indicating the reaction proceeds mainly through a direct mechanism. The strong Fermi resonance between the (020) and (100) vibrationally excited states makes it hard to define their efficacy for reactivity, although it is conceivable that the bending excitation is much more effective than the symmetric excitation according to the geometry of the transition state in the entrance channel.

1. Introduction

The endothermic reaction $H + CO_2 \rightarrow OH + CO$, and its reverse, play vital roles in atmospheric [1], combustion [2], and interstellar chemistry [3,4]. They proceed via the intermediate HOCO complex supported by the *trans* and *cis* deep wells in between two near-isoenergetic barriers in the entrance and exit channels, representing a prototype for complex-forming four-atom reactions as $H_2+OH \rightarrow H + H_2O$ for direct four-atom reactions. Over the years, many experimental studies have been devoted to the title reaction for dynamical and kinetic properties. Reactive cross sections and product state distributions were measured with the hydrogen atoms being produced in the photolysis of a HX molecule (X = Cl, Br, or I) [5–8]. The measured thermal rate constants of the $OH + CO \rightarrow H + CO_2$ reaction show a strong non-Arrhenius behavior. They are nearly independent on temperature between 80 and 500 K, but increase sharply with temperature above 500 K [9–11]. On the contrary, the measured thermal rate constants of the title reaction exhibit a clear Arrhenius behavior. The real-time clocking of the title reaction is in the subpicosecond range according to the photodissociation experiments of weakly bound van der Waals complexes [12–14].

Theoretically, extensive studies have been carried out for the HOCO system. In 1987, the first global analytic potential energy surface (PES) was constructed by Schatz and coworkers (denoted as SFH) based on a relatively small number of *ab initio* points and the many-body expansion approach. Following that, a few more PESs have been constructed and widely used for dynamics studies, such as the KSW, BS, YMS, LTSH, and VvHK PES [15–20], but the accuracy of the PESs were still not ideal. The situation has been greatly improved, thanks to new PESs based on large numbers of high-level *ab initio* points and more accurate fitting methods. In 2012, Li et al. developed a global PES and its modified version [21,22] using the permutation invariant polynomial (PIP) method [23]. Subsequently, Chen et al. reported independently another PES using the neural network (NN) method [24], with data points spreading in a more complete configuration space [25]. It was shown that the NN PES fits the *ab initio* points considerably better than the PIP PES. In 2014, Li et al. reported a new full-dimensional global PES based on the same *ab initio* data set generated by Chen et al. [25], but fit using the newly proposed permutation invariant polynomial-neural network (PIP-NN) method [26,27], representing the most accurate PES so far for the HOCO system [28].

Schatz and co-workers performed pioneering quasi-classical trajectory (QCT) calculations for the $H + CO_2 \rightarrow OH + CO$ reaction on different PESs [15,17,29]. In 2012, QCT calculations on the PIP PES [21] reproduce for the first time the monotonically increasing integral cross section (ICS) with collision energy observed in the experiment for the reaction. The calculated thermal rate constants on this PES are also in good agreement with experimental ones [30]. Subsequently, Valero and coworkers carried out a QCT study of the title reaction on a new interpolated PES based on the M06-2X density functional. The total reaction cross sections reveal

* Corresponding authors.
E-mail addresses: liushu1985@dicp.ac.cn (S. Liu), zhangdh@dicp.ac.cn (D.H. Zhang).

http://dx.doi.org/10.1016/j.cplett.2017.02.083
0009-2614/

quantitative agreement with experiment in the whole range of relative translational energies 1.2–2.5 eV [31].

The HOCO system presents a huge challenge to quantum dynamics. The combination of a relatively long-lived collision complex and three heavy atoms in the reaction makes the rigorous quantum scattering calculations extremely difficult. Full-dimensional quantum dynamical studies of the $HOCO^-$ and HCO_2^- photodetachment were performed on the LTSH and PIP-NN PESs [32–35]. Extensive quantum mechanical (QM) studies were carried out for the total reaction probabilities and rate constants on different PESs for the OH + CO → H + CO_2 reaction [36–40,28]. In 2012, we performed a full-dimensional state-to-state quantum dynamics calculation for total angular momentum $J = 0$ on LTSH and PIP-NN PESs for the OH + CO reaction [41–43], representing the first state-to-state quantum study of a complex forming four-atom reaction. Despite the significant progress on OH + CO reaction, the quantum dynamical study for the reverse reaction has remained a challenge.

In this letter, we report a time-dependent wave packet (TDWP) calculation of the title reaction in full dimensions on the PIP-NN PES. To the best of our knowledge, this is the first QM calculation for the title reaction. We calculated the total reaction probabilities from the ground rovibrational initial state and some vibrationally excited states for the total angular momentum $J = 0$. The total reaction probabilities for some $J > 0$ were also computed under the centrifugal sudden (CS) approximation, and were used to yield ICS for the ground initial state.

2. Theory

We outline the theory of the TDWP method for calculating the initial state selected total reaction probability for a atom-triatom reaction H + CO_2 → OH + CO in full dimensions. For details, please refer to our early works [44]. The Hamiltonian expressed in the reactant Jacobi coordinates shown in Fig. 1 for a given total angular momentum J can be written as

$$H = -\frac{\hbar^2}{2\mu}\frac{\partial^2}{\partial R^2} + h_1(r_1) + h_2(r_2) + \frac{(\mathbf{J}-\mathbf{j}_{12})^2}{2\mu R^2} + \frac{\mathbf{j}_1^2}{2\mu_1 r_1^2} + \frac{\mathbf{j}_2^2}{2\mu_2 r_2^2} + V(R, r_1, r_2, \theta_1, \theta_2, \varphi), \quad (1)$$

where μ is the reduced mass between the center-of-mass of H and CO_2, $\mathbf{J}$ is the total angular momentum operator of the system, $\mathbf{j}_{12}$ is the total angular momentum operator of CO_2, $\mathbf{j}_2$ is the rotational angular momentum operator of CO, and $\mathbf{j}_1 = \mathbf{j}_{12} - \mathbf{j}_2$ is the orbital angular momentum of CO_2. The diatomic reference Hamiltonian $h_i(r_i)$ (i = 1,2) is defined as

$$h_i(r_i) = -\frac{\hbar^2}{2\mu_i}\frac{\partial^2}{\partial r_i^2} + V_i(r_i). \quad (2)$$

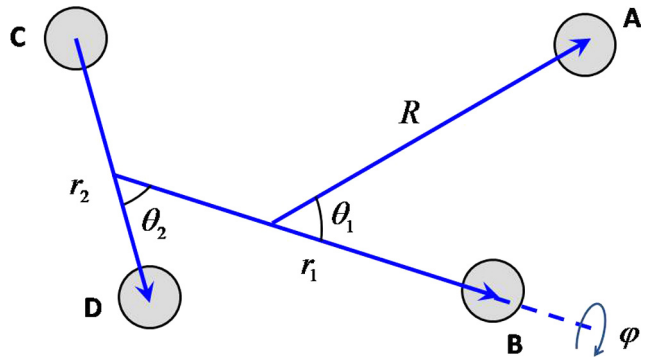

Fig. 1. The reagent Jacobi coordinates $(R, r_1, r_2, \theta_1, \theta_2, \varphi)$ for the H + CO_2 atom-triatom reaction.

The time-dependent wave function can be expanded in terms of the translational basis of R, the vibrational basis $\phi_{v_i}(r_i)$, and the body-fixed (BF) rovibrational eigenfunction as

$$\Psi^{JM\epsilon}_{v_0 j_0 K_0}(\mathbf{R}, \mathbf{r_1}, \mathbf{r_2}, t) = \sum_{n,v,j,K} F^{JM\epsilon}_{nvjK,v_0 j_0 K_0}(t) u_n^{v_1}(R)\phi_{v_1}(r_1)\phi_{v_2}(r_2)\mathcal{Y}^{JM\epsilon}_{jK}(\hat{R}, \hat{r}_1, \hat{r}_2). \quad (3)$$

The BF total angular momentum eigenfunctions can be written as,

$$\mathcal{Y}^{JM\epsilon}_{jK} = (1+\delta_{K0})^{-1/2}\sqrt{\frac{2J+1}{8\pi}}[D^{J*}_{K,M}Y^{j_{12}K}_{j_1 j_2} + \epsilon(-1)^{j_1+j_2+j_{12}+J}D^{J*}_{-K,M}Y^{j_{12}-K}_{j_1 j_2}] \quad (4)$$

$$\equiv \mathcal{D}^{J*}_{K,M}Y^{j_{12}K}_{j_1 j_2} + \epsilon(-1)^j\mathcal{D}^{J*}_{-K,M}Y^{j_{12}-K}_{j_1 j_2} \quad (5)$$

where $D^J_{K,M}(\Theta\Phi\Psi)$ is the Wigner rotation matrix [45] with three Euler angles $(\Theta\Phi\Psi)$, ϵ is the parity of the system defined as $\epsilon = (-1)^{j_1+j_2+L}$ with $\mathbf{L} = \mathbf{J} - \mathbf{j_{12}}$ being the orbital angular momentum of H and CO_2, and $Y^{j_{12}K}_{j_1 j_2}$ is the angular momentum eigenfunction of $\mathbf{j}_{12}$ defined as,

$$Y^{j_{12}K}_{j_1 j_2} = \sum_m D^{j_{12}*}_{Km}(\chi, \theta_1, \varphi)\sqrt{\frac{2j_1+1}{4\pi}}\langle j_2 m j_1 0|j_{12}m\rangle y_{j_2 m}(\theta_2, 0) \quad (6)$$

where y_{jm} are spherical harmonics. Note that in Eq. (4), the restriction $\epsilon(-1)^{j_1+j_2+j_{12}+J} = 1$ for $K = 0$ partitions the whole rotational basis set into even and odd parities. Thus a $K = 0$ initial state can only appear in one of these two parity blocks. For $K > 0$, however, there is no such restriction, the basis set is the same for even and odd parities. Hence a $K > 0$ initial state can appear in both parities.

We construct an initial wave packet $\psi_i(0)$ and propagate it using the split-operator method. The total reaction probability for that specific initial state i for a whole range of energies can be obtained by evaluating the reactive flux

$$P_i^R(E) = \frac{\hbar}{m_s}\,\mathrm{Im}[\langle\psi^+_{iE}|\delta(s-s_0)\frac{\partial}{\partial s}|\psi^+_{iE}\rangle], \quad (7)$$

where s is the coordinate perpendicular to a dividing surface located at s_0. ψ^+_{iE} denotes the time-independent (TI) wavefunction, which can be obtained by performing a Fourier transform of the time-dependent wave function as

$$|\psi^+_{iE}\rangle = \frac{1}{a_i(E)}\int_{-\infty}^{\infty} e^{\frac{i}{\hbar}(E-H)t}|\psi_i(0)\rangle dt. \quad (8)$$

The coefficient $a_i(E)$ is the overlap between the initial wave packet and the energy-normalized asymptotic scattering function, $a_i(E) = \langle\phi_{iE}|\psi_i(0)\rangle$.

The numerical parameters for the wave packet propagation were as follows: the interaction region was defined by a rectangular box of [2.0,7.0] a_0 in the r_1 coordinate, and [1.5,6.5] a_0 for the R coordinate. The number of vibrational basis functions used was 100 for the r_1 coordinate. For the R coordinate, we used 36 sine discrete variable representation (DVR) points. The asymptotic region was defined from 6.5 to 11.5 a_0 with 36 sine DVR points for the R coordinate and 10 vibrational basis functions for the r_1 coordinates. The number of vibrational basis functions for the nonreactive CO is 8. For the rotational motion, we used $j_{max} = 95$ and $l_{max} = 110$, which results in 369,376 rotational basis functions for $K = 0$ and even parity. The initial Gaussian wave packet was centered at $R_0 = 10.0a_0$ with a narrow width of 0.3 a_0, and a central energy of 1.7 eV. A dividing surface is placed at $r_1 = 5.5a_0$ to extract probabilities. The wave-packet propagation was carried out using a time increment of 10 a.u. Since there are two equivalent product channels in the reaction, we treat the OC' bond as a

nonreactive bond in this work, which has been demonstrated to be a very good approximation in describing the H + H_2O and the title abstraction reaction. The reaction probabilities should be multiplied by a factor of 2, if compared with experimental results.

We employed the PIP-NN PES in our calculations, which is fitted by using 74,400 *ab initio* points at the UCCSD(T)-F12a/aug-cc-pVTZ level of theory [28]. The PES is quite complex, involving two bottlenecks and two complex wells, as shown in Fig. 2. The reaction between H and CO_2 proceeds through a tight transition state (TS2) with a static barrier height of 1.09 eV.

3. Results and discussion

Fig. 3 shows the convergence of total reaction probabilities for the ground initial state for $J = 0$ with respect to the propagation time. At short propagation time, the reaction probabilities are smooth as a function of collision energy, and increase with the propagation time very quickly, in particular for high collision energies. At $T = 4800$ a.u., the reaction probability at $E_c = 2.4$ eV reaches 0.01 (the final converged value is 0.016). With the increase of propagation time, the reaction probabilities increase steadily, but slower than the early time. At the mean time, oscillatory structures begin to appear as can be seen from the $T = 9000$ a.u. curve. With the further increase of propagation time, the reaction probability gradually reaches its final converged value, and oscillatory structures become increasingly rich. The reaction probabilities are essentially converged after the wave packet is propagated for about 30,000 a.u., as compared to the 45,000 a.u. and 72,000 a.u. curves. This propagation time is much shorter than that reported earlier for the OH + CO reaction (450,000 a.u.).

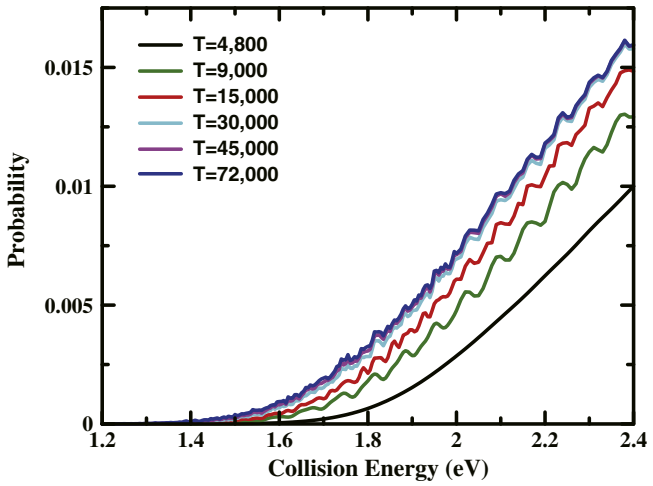

Fig. 3. Total reaction probabilities for the ground initial state of the H + CO_2 reaction on the PIP-NN PES at wave packet propagation time of $T = 4800$, 9000, 15,000, 30,000, 45,000, and 72,000 a.u.

The converged total reaction probability for the ground initial state is small in the entire collision energy region considered here. It has a threshold energy of ~ 1.4 eV, slightly higher than

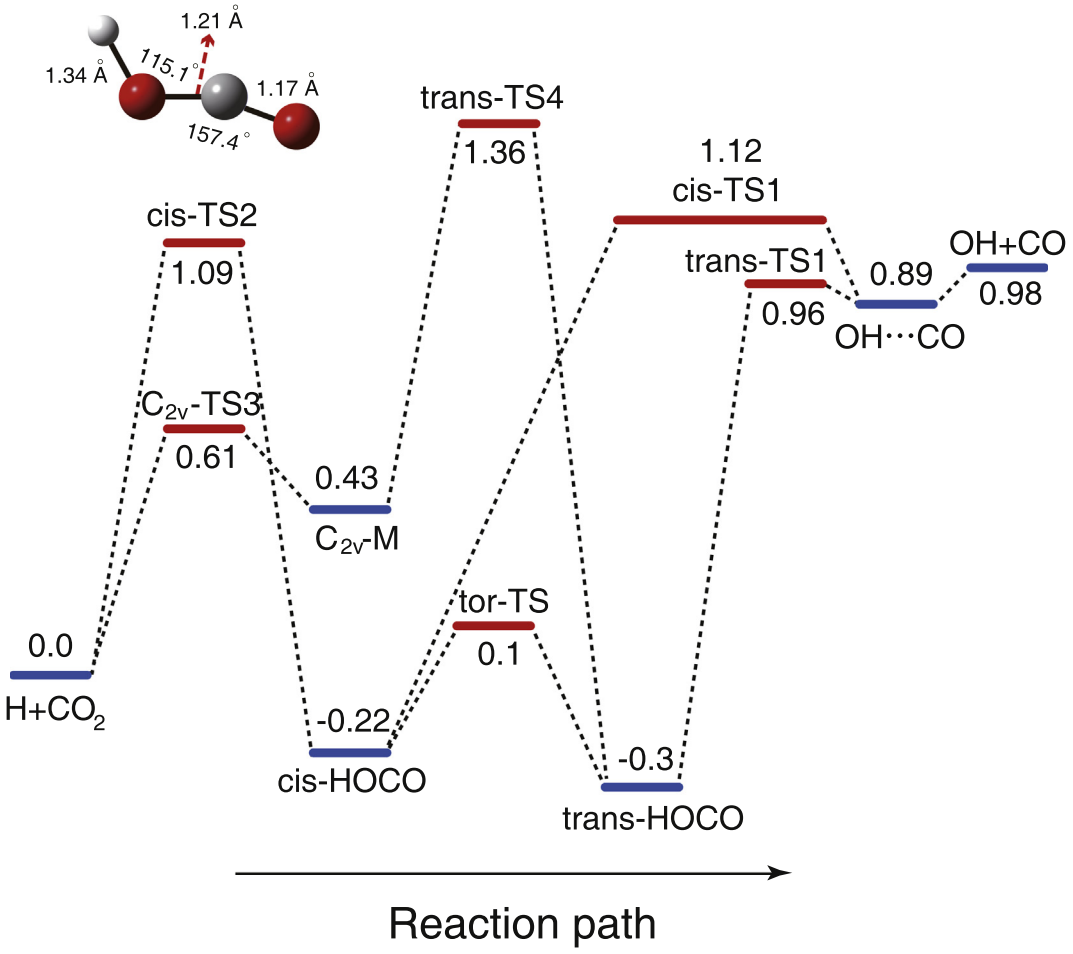

Fig. 2. Energetic of reaction pathways for the H + CO_2 → OH + CO reaction. The *ab initio* energies of the stationary points are given in eV. The zero of the energy is corresponding to the ground state CO_2.

the zero-point corrected barrier height of 1.12 eV of the cis-TS2 transition state, and reaches a value of 0.016 at E_c = 2.4 eV. There are many oscillatory structures, but far less pronounced than those observed for the reverse reaction [43]. The relatively short propagation time and weak oscillatory structures in the total reaction probabilities indicate that the reaction proceeds mainly through a direct mechanism. After passing the cis-HOCO TS2 transition state, the majority of the wave function is not trapped in these two cis-HOCO and trans-HOCO wells, very likely passes directly the cis-TS1 transition state in the exit channel, yielding the reaction products. Only a tiny portion of the wave function is trapped in the wells, giving raise to the tiny oscillatory structures in reaction probabilities.

Fig. 4(a) shows the total reaction probabilities for three vibrationally excited initial states for the total angular momentum $J = 0$ as a function of the collision energy, together with the ground initial state. All these three vibrational excitations reduce the reaction threshold energy and enhance the reactivity, with the state with 1388 cm^{-1} excitation energy to be most effective. Despite its highest excitation energy, the asymmetric (001) excitation is least effective on prompting the reaction. For CO_2, because the symmetric stretching vibrational frequency v_1 is very close to the double of the bending frequency v_2, there are strong Fermi resonances between them, leading to the vibrational states with excitation energy of 1284 cm^{-1} and 1388 cm^{-1} being the mixture of (100) and (02^00). By using the method proposed by one of the authors [46], we decoupled Fermi resonant wavefunctions back to 'pure' uncoupled vibrational wavefunctions, and determined the mixing coefficients for the Fermi resonant pair to be:

$$\psi_{1284cm^{-1}} = 0.67\psi^0_{02^00} + 0.74\psi^0_{100}, \quad (9)$$
$$\psi_{1388cm^{-1}} = -0.74\psi^0_{02^00} + 0.67\psi^0_{100}.$$

As seen, the 1284 cm^{-1} and 1388 cm^{-1} states are more or less equally mixed by the (100) and (02^00) states, with the 1388 cm^{-1} state possessing a slightly larger component of the (02^00) state. However, the 1388 cm^{-1} is much more effective on prompting the reaction. We anticipate that the approaching of H atom to CO_2 lifts the degeneracy of the (100) and (02^00) states, and the 1388 cm^{-1} state evolves more to the (02^00) state. As shown in the results, the 1388 cm^{-1} state carrying more (02^00) component is much more reactive than the 1284 cm^{-1} state. As can be seen from Fig. 2, at the cis-TS2 transition state the O–C–O bending angle is 157.4°, substantially away from the collinear geometry of CO_2, while the breaking C–O bond length is 1.21 Å, rather close to the equilibrium value for CO_2 of 1.16 Å. As a result, the bending excitation is substantially more effective on promoting the reaction than stretching excitations. This is also in accordance with the sudden vector projection (SVP) model proposed by Guo and co-workers [47,48]. The bending and symmetric induced enhancements for the title reaction are also consistent with the observations in the reverse OH + CO and HCO_2^- reactions on the same PIP-NN PES [43,35]: that the CO_2 product are dominantly excited in bending and symmetric modes, and there is essentially no antisymmetric stretching excitation of the CO_2 products.

In Fig. 4(b), we show all the probabilities as a function of total energy measured with respect to the ground state energy of CO_2. As can be seen the vibrational energy initially deposited in the 1284 cm^{-1} and 1388 cm^{-1} states has a larger efficacy than the translational energy on prompting the reaction. In contrast, the asymmetric (001) excitation is less effective than the translational energy.

With huge basis sets and quite long wave packet propagation time used in the calculation, it is not feasible at present to calculate the total reaction probabilities for $J > 0$ with sufficient number of K blocks included as the computational effort increases by a factor of $2 * NK + 1$ (where NK is the number of K-blocks). The CS approximation was employed to calculate the total reaction probabilities for $J > 0$ with only $K = 0$ block included, from which ICS can be obtained. Fig. 5 shows the CS ICS for the ground initial state as a

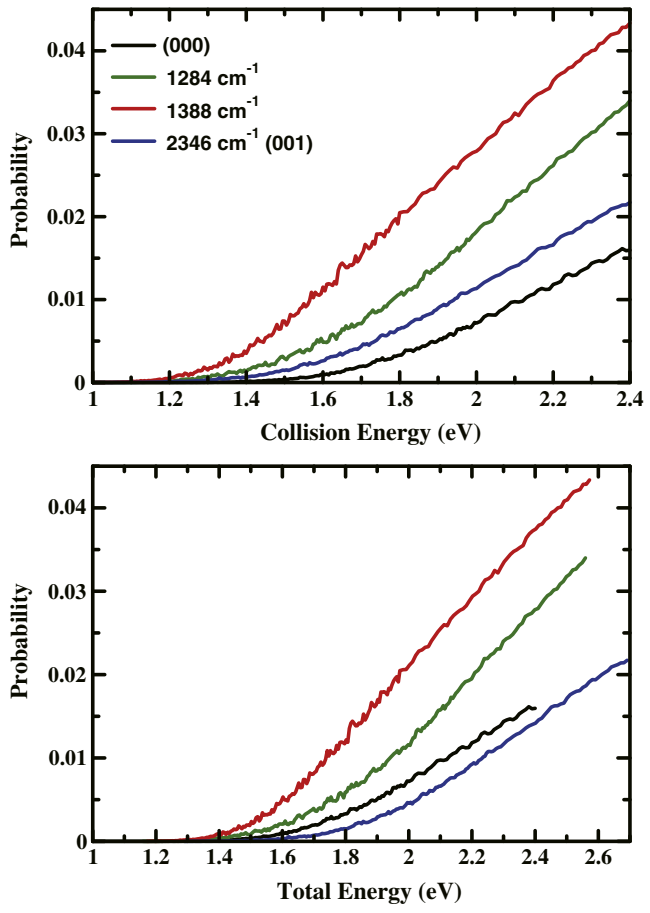

Fig. 4. Total reaction probabilities for the ground and three low-lying vibrationally excited states of CO_2 as a function of the collision energy (a), and as a function of the total energy (b).

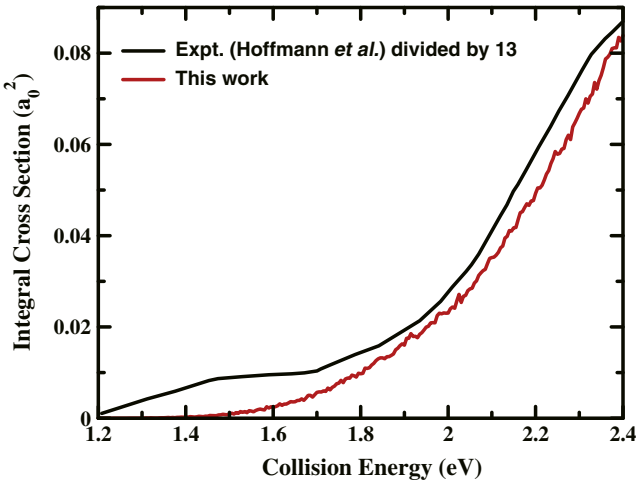

Fig. 5. CS total ICS for the ground initial state of the H + CO_2 reaction as a function of the collision energy.

function of the collision energy. The total ICS increases monotonically with the collision energy, consistent with experimental observations. However, the absolute magnitude is substantially smaller in the whole energy range than the experimental data of Hoffmann [8] (by roughly a factor of 15) and previous QCT results on the LTSH and CCSD-3/d PES [29,30]. We believe the CS approximation employed in our calculation is the main reason for the huge discrepancy between the experiment and present calculation. In addition, the ICSs presented here are only for the ground rotational state, while the experimental results contain the contributions from all the rotational states populated in the experiment. Further studies should be performed to investigate the effects of initial rotational excitation of reagent on the reactions, although QCT calculations on the CCSD-3/d PES revealed that rotation excitation of reagent only has a relatively small effect on the reactivity. Because the previous QCT calculations were performed on different PES, it is hard to justify whether the large discrepancy on ICS between the present calculation and previous QCT calculation originates from the PES or dynamics method.

4. Conclusions

A full dimensional quantum dynamics calculation has been carried out to study the prototypical complex forming H + CO_2 → OH + CO reaction. It is found that the total reaction probabilities for the ground and a few vibrationally excited states can be converged with a propagation time much short than that for the reverse OH + CO reaction, only exhibit very small oscillatory structures, indicating the reaction proceeds mainly through a direct mechanism. After passing the cis-TS2 transition state in entrance channel, the majority of wave function passes directly one of the two TS1 transition states in the exit channel, yielding the reaction products. It would be interesting to carry out detailed trajectory calculations to find out through which transition state in the exit channel the products are produced.

All the vibrational excitations can enhance the reactivity, but their efficacy are very different. The asymmetric stretch excitation is less effective than the translational energy on promoting the reaction. The strong Fermi resonance between the symmetric stretch and the second bending excited state results in two states with 1284 cm^{-1} and 1388 cm^{-1} excitation energies. The 1388 cm^{-1} state possesses a slightly larger component of the $(02^{0}0)$ state, but is much more effective on prompting the reaction than the 1284 cm^{-1} state. According to the geometry of the cis-TS2 transition state, it is conceivable that the bending excitation is much more effective than the symmetric excitation. We anticipate that the approaching of H atom to CO_2 lifts the degeneracy of the (100) and $(02^{0}0)$ states, and the 1388 cm^{-1} state evolves more to the $(02^{0}0)$ state, making it more effective on promoting the reaction.

The calculated ICSs with the CS approach are substantially smaller than the experimental measurements, and previous QCT results on the LTSH and CCSD-3/d PES. It is likely that the CS approximation does not work well for the reaction, further quantum dynamics calculation with sufficient number of K blocks included should be carried out. At the mean time, theoretical investigations on the effects of initial rotation excitations on the reaction are necessary to make the comparison between theory and experiment more closely.

Acknowledgements

This work was supported by the National Natural Science Foundation of China (Grant Nos. 21403223, 21433009, 21590804), the Ministry of Science and Technology of China (2013CB834601), DICP (Grant: DICP ZZBS201611), and the Chinese Academy of Sciences (XDB17010000).

References

[1] B.J. Finlayson-Pitts, J.N. Pitts, Chemistry of the Upper and Lower atmosphere, Academic press, San Diego, 2000.
[2] J.A. Miller, R.J. Kee, C.K. Westbrook, Annu. Rev. Phys. Chem. 41 (1990) 345.
[3] T.P.M. Goumans, M.A. Uppal, W.A. Brown, Mon. Not. R. Astron. Soc. 384 (2008) 1158.
[4] S. Ioppolo, Y. van Boheemen, H.M. Cuppen, E.F. van Dishoeck, H. Linnartz, Mon. Not. R. Astron. Soc. 413 (2011) 2281.
[5] K. Kleinermans, J. Wolfrum, Lasers Chem. 2 (1983) 339.
[6] A. Jacobs, M. Wahl, R. Weller, J. Wolfrum, Chem. Phys. Lett. 158 (1989) 161.
[7] Y. Chen, G. Hoffmann, D. Oh, C. Wittig, Chem. Phys. Lett. 159 (1989) 426.
[8] G. Hoffmann, D. Oh, Y. Chen, Y.M. Engel, C. Wittig, Isr. J. Chem. 30 (1990) 115.
[9] A.R. Ravishankara, R.L. Thompson, Chem. Phys. Lett. 99 (1983) 377.
[10] M.J. Frost, P. Sharkey, I.W.M. Smith, Faraday Discuss. Chem. Soc. 91 (1991) 305.
[11] D.M. Golden et al., J. Phys. Chem. A 102 (1998) 8598.
[12] C. Wittig, S. Sharpe, R.A. Beaudet, Acc. Chem. Res. 21 (1988) 341.
[13] N.F. Scherer, C. Sipes, R.B. Bernstein, A.H. Zewail, J. Chem. Phys. 92 (1990) 5239.
[14] S.I. Ionov, G.A. Brucker, C. Jaques, L. Valachovic, C. Wittig, J. Chem. Phys. 97 (1992) 9486.
[15] G.C. Schatz, M.S. Fitzcharles, L.B. Harding, Faraday Discuss. Chem. Soc. 84 (1987) 359.
[16] K. Kudla, G.C. Schatz, A.F. Wagner, J. Chem. Phys. 95 (1991) 1635.
[17] K.S. Bradley, G.C. Schatz, J. Chem. Phys. 106 (1997) 8464.
[18] H.G. Yu, J.T. Muckerman, T.J. Sears, Chem. Phys. Lett. 349 (2001) 547.
[19] M.J. Lakin, D. Troya, G.C. Schatz, L.B. Harding, J. Chem. Phys. 119 (2003) 5848.
[20] R. Valero, M.C. van Hemert, G.J. Kroes, Chem. Phys. Lett. 393 (2004) 236.
[21] J. Li et al., J. Chem. Phys. 136 (2012) 041103.
[22] J. Li et al., J. Phys. Chem. A 116 (2012) 5057.
[23] J.M. Bowman, G. Czakó, B. Fu, Phys. Chem. Chem. Phys. 13 (2011) 8094.
[24] J. Behler, Phys. Chem. Chem. Phys. 13 (2011) 17930.
[25] J. Chen, X. Xu, D.H. Zhang, J. Chem. Phys. 138 (2013) 221104.
[26] B. Jiang, H. Guo, J. Chem. Phys. 139 (2013) 054112.
[27] J. Li, B. Jiang, H. Guo, J. Chem. Phys. 139 (2013) 204103.
[28] J. Li, J. Chen, D.H. Zhang, H. Guo, J. Chem. Phys. 140 (2014) 044327.
[29] D. Troya, M.J. Lakin, G.C. Schatz, L.B. Harding, M. Gonzalez, J. Phys. Chem. B 106 (2002) 8148.
[30] C. Xie, J. Li, D. Xie, H. Guo, J. Chem. Phys. 137 (2012) 024308.
[31] R. Valero, S. Andersson, Phys. Chem. Chem. Phys. 14 (2012) 16699.
[32] S. Zhang, D.M. Medvedev, E.M. Goldfield, S.K. Gray, J. Chem. Phys. 125 (2006) 164312.
[33] J. Ma, H. Guo, Chem. Phys. Lett. 511 (2011) 193.
[34] J. Wang, J. Li, J. Ma, H. Guo, J. Chem. Phys. 140 (2014) 184314.
[35] L. Zou, J. Li, H. Wang, J. Ma, H. Guo, J. Phys. Chem. A 119 (2015) 7316.
[36] D.H. Zhang, J.Z.H. Zhang, J. Chem. Phys. 103 (1995) 6512.
[37] R. Valero, D.A. McCormack, G.J. Kroes, J. Chem. Phys. 120 (2004) 4263.
[38] D.M. Medvedev, S.K. Gray, E.M. Goldfield, M.J. Lakin, D. Troya, G.C. Schatz, J. Chem. Phys. 120 (2004) 1231.
[39] S. Liu, X. Xu, D.H. Zhang, Theor. Chem. Acc. 131 (2012) 1068.
[40] J. Ma, J. Li, H. Guo, J. Phys. Chem. Lett. 3 (2012) 2482.
[41] S. Liu, X. Xu, D.H. Zhang, J. Chem. Phys. 135 (2011) 141108.
[42] C. Wang, S. Liu, D.H. Zhang, Chem. Phys. Lett. 537 (2012) 16.
[43] S. Liu, J. Chen, B. Fu, D.H. Zhang, Theor. Chem. Acc. 133 (2014) 1558.
[44] D.H. Zhang, J.C. Light, J. Chem. Phys. 104 (1996) 4544.
[45] M.E. Rose, Elementary Theory of Angular Momentum, John Wiley, New York.
[46] H. Tang, D.H. Zhang, Chem. Phys. Lett. 265 (1997) 84.
[47] B. Jiang, H. Guo, J. Chem. Phys. 138 (2013) 234104.
[48] B. Jiang, H. Guo, J. Am. Chem. Soc. 135 (2013) 15251.